COMPDYN 2011
ECCOMAS Thematic Conference on
Computational Methods in Structural Dynamics and Earthquake Engineering
M. Papadrakakis, M. Fragiadakis, V. Plevris (eds.)
Corfu, Greece, 25-28 May 2011

IDENTIFICATION AND SIZING OF DEFECTS IN PIPELINES BY THE WAVE FINITE ELEMENT METHOD USING TORSIONAL GUIDED WAVES

M. Kharrat, W. Zhou, O. Bareille, M. Ichchou

Laboratoire de Tribologie et Dynamique des Systèmes, Ecole Centrale de Lyon,
36 Avenue Guy de Collongue 69134 Ecully Cedex, France
E-mails: mohamed.kharrat@ec-lyon.fr, zhou.wenjin@ec-lyon.fr, olivier.bareille@ec-lyon.fr,
mohamed.ichchou@ec-lyon.fr

Keywords: Guided waves, Reflection coefficient, Damage identification, Defect sizing, Wave finite element method, Torsional wave.

Abstract. *Structural health monitoring of pipelines by guided waves is a technique under continuous development. It proved a relevant efficiency in defects detection in pipes. The analysis of reflections from cracks provides guidance to defects sizing. A guided wave technique capable of screening long lengths of pipes has been developed in our laboratory. The wave finite element method, adapted for the case of hollow cylinders as waveguide, was used to calculate reflection coefficients from different rectangular notches sizes and some singularities located in industrial pipeline. The numerical simulations were established while varying the excitation frequency. The aim of this work is to create a database for the identification and approximation of defects sizes detected in an industrial installation subject of experimental tests. The results were compared to usual finite element simulations in order to validate the technique. Good agreement was found between the results. Thus, the database can be used to size approximately the founded defects.*

1 INTRODUCTION

The technique of defect detection by guided-waves is the solution that becomes more and more widespread in the non-destructive testing field. This technique allows the scanning of long-distance pipeline from a single position through the use of guided-waves propagation along the tested pipes and facilitates the defect detection. Torsional mode has shown relevant advantages in defect detection in pipes [1, 2]. These found damages need to be dimensioned in order to be classified depending on its severity. The reflection and transmission of the wave through defects gives good information about its sizes. Indeed, guided wave reflection and transmission depends on the defect size and shape, as well as the incident wave type and frequency. Since the near field is complex due to the presence of defects, analytical model can not readily be used to describe the near field effect that accounts for the energy redistribution of the scattered wave modes. Structural waveguides usually consist of many local features, such as welding, ribs, curved members, supports and others. They could also largely destroy the original wave form and evoke spurious echoes.

Wave propagation in waveguides has been studied for a long time as far as the question of propagation through periodic structures was addressed [3, 4]. The Wave Finite Element Method (WFEM) was employed for the low and midfrequency description of coupled structures and the analysis of wave propagation through a notch was studied [5]. Other studies consider the applicability of the WFEM and study the guided elastic wave propagation in cylindrical pipes with local inhomogeneities [6]. The intact and damaged curved structures was also treated to determine their response to incident waves [7].

In this paper, we present firstly the basis of the WFEM. This latter was then used to construct a database of reflection coefficients from a rectangular notch in pipe with three dimensions : depth, axial and circumferential extents. The chosen mode was the torsion and calculations was made in the frequency range $[5 - 15]kHz$.

2 WAFE FINITE ELEMENT METHOD

In this section, we present the basis of the WFEM that was used to construct a database of reflection coefficients from defects and features in the pipe. A hybrid WFE/FE method was employed for the scattered field calculation [6].

By using axisymmetric elements, WFE method for the 1-D wave propagation problem is employed to extract the wave numbers and mode shapes for axisymmetric modes (longitudinal modes L(0, m) and torsional modes T(0, m)). Those eigenmodes are then superposed to form a scattering equation by connecting with FE formulation of the pipe segment with inhomogeneities. The dynamic reduction technique, component modal synthesis (CMS) is combined to formulate a numerically efficient scattering equation when dealing with the complex substructure models. This reduction technique fully takes into account the fact that the pipelines usually have some standard local features, and also allows various types of 3-D defects to be considered with ease.

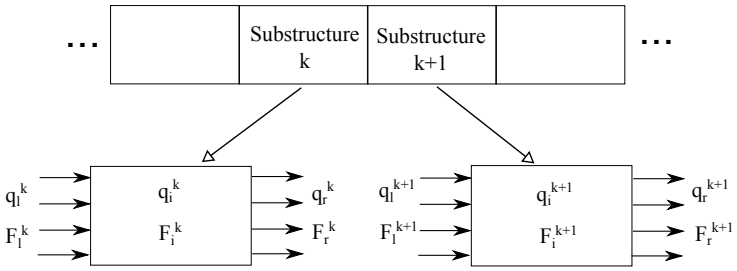

Figure 1: Structure discretized to identical cells

2.1 Finite element description

The structure can be discretized to identical cells as is shown in figure 1. The general FE formulation of a typical cell for the 1-D wave propagation in the pipe can be written as

$$\begin{bmatrix} \mathbf{D}_{ll} & \mathbf{D}_{li} & \mathbf{D}_{lr} \\ \mathbf{D}_{il} & \mathbf{D}_{ii} & \mathbf{D}_{ir} \\ \mathbf{D}_{rl} & \mathbf{D}_{ri} & \mathbf{D}_{rr} \end{bmatrix} \begin{Bmatrix} \mathbf{q}_l \\ \mathbf{q}_i \\ \mathbf{q}_r \end{Bmatrix} = \begin{Bmatrix} \mathbf{F}_l \\ \mathbf{F}_i \\ \mathbf{F}_r \end{Bmatrix}, \tag{1}$$

where [D] is the structure dynamic stiffness matrix, subscripts *l*, *r* and *i* denote the left, right and interior components, respectively. Assume that no external force be applied at interior dofs, eq.1 is condensed as

$$\begin{bmatrix} \mathbf{S}_{ll} & \mathbf{S}_{lr} \\ \mathbf{S}_{rl} & \mathbf{S}_{rr} \end{bmatrix} \begin{Bmatrix} \mathbf{q}_l \\ \mathbf{q}_r \end{Bmatrix} = \begin{Bmatrix} \mathbf{F}_l \\ \mathbf{F}_r \end{Bmatrix}, \tag{2}$$

where

$$\begin{aligned} \mathbf{S}_{ll} = \mathbf{D}_{ll} - \mathbf{D}_{li}{\mathbf{D}_{ii}}^{-1}\mathbf{D}_{il}\ ; \quad \mathbf{S}_{lr} = \mathbf{D}_{lr} - \mathbf{D}_{li}{\mathbf{D}_{ii}}^{-1}\mathbf{D}_{ir}\ ; \\ \mathbf{S}_{rl} = \mathbf{D}_{rl} - \mathbf{D}_{ri}{\mathbf{D}_{ii}}^{-1}\mathbf{D}_{il}\ ; \quad \mathbf{S}_{rr} = \mathbf{D}_{ri} - \mathbf{D}_{ri}{\mathbf{D}_{ii}}^{-1}\mathbf{D}_{ir}. \end{aligned}$$

To describe the wave motion, eigensolution need to be decomposed to positive and negative going wave modes for the computational purpose. These modes include both the propagating and non-propagating modes. Through the eigensolutions, the non-reflecting boundaries are described by the incident wave mode bases

$$\mathbf{q}_r = [\mathbf{q}^+]\mathbf{A}^+, \quad \mathbf{F}_r = -[\mathbf{F}^+]\mathbf{A}^+. \tag{3}$$

Substitution into Equation 2 yields

$$\left\{(\mathbf{S}_{rl}\mathbf{S}_{ll}^{-1}\mathbf{S}_{lr} - \mathbf{S}_{rr})[\mathbf{q}^+] - [\mathbf{F}^+]\right\}\mathbf{A}^+ = \mathbf{S}_{rl}\mathbf{S}_{ll}^{-1}\mathbf{F}_l. \tag{4}$$

From Equation 4, the excited wave modes can be calculated for a given excitation. The wave field is thus represented fully by the incident wave modes.

The eigenmodes in the structural waveguide that come from the spectral solutions of WFE method can be superposed to describe the wave field. Those eigenmodes travel independently and do not interfere with one another. A set of wave modes can be traveling at the same time in the waveguides, thus the motion at any point therein is simply regarded as the sum of the motion of various modes. The incident, reflected and transmission waves can be expressed as

$$\mathbf{q}^{inc} = [\mathbf{q}^+]\Lambda^+\mathbf{A}^{inc}, \quad \mathbf{q}^{ref} = [\mathbf{q}^-]\Lambda^-\mathbf{A}^{ref}, \quad \mathbf{q}^{tra} = [\mathbf{q}^+]\Lambda^+\mathbf{A}^{tra}, \tag{5}$$

where $\mathbf{q}^{inc}$ and $\mathbf{q}^{tra}$ are formed of the same bases, $[\mathbf{q}^{+}]$ and $[\mathbf{q}^{-}]$ are normalized N by N_r matrices, $\mathbf{A}^{inc}$, $\mathbf{A}^{ref}$ and $\mathbf{A}^{tra}$ denote the amplitudes of the corresponding waves, Λ^{+} and Λ^{-} are diagonal matrices relating respectively to the positive and negative going waves, which are given as

$$\Lambda^{\pm} = diag\left\{e^{\pm jk_i x}\right\}, (i = 1, 2, ...N_r). \tag{6}$$

Analogically, we can obtain the expressions of $\mathbf{F}^{inc}$, $\mathbf{F}^{ref}$ and $\mathbf{F}^{tra}$:

$$\mathbf{F}^{inc} = [\mathbf{F}^{+}]\Lambda^{+}\mathbf{A}^{inc}, \quad \mathbf{F}^{ref} = [\mathbf{F}^{-}]\Lambda^{-}\mathbf{A}^{ref}, \quad \mathbf{F}^{tra} = [\mathbf{F}^{+}]\Lambda^{+}\mathbf{A}^{tra}, \tag{7}$$

where the force vectors are also eigenvectors or obtained from the displacement vectors.

2.2 Wave propagation in an infinite structural waveguide with a local defect

Consider an infinitely long structure with the local inhomogeneities which are due to the geometry or material variation. A monochromatic incident wave, which comprises a single or multiple wave modes, is assumed to be generated at $x - \infty$ and travel in the positive $x - \infty$ direction. Scattering phenomenon emerges when the incident wave impinges on those inhomogeneities as is shown in figure 2.

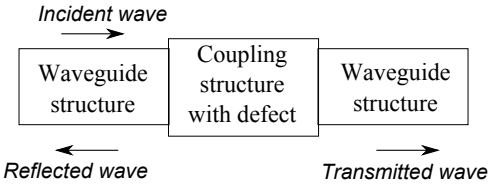

Figure 2: Waves propagation through damaged coupling structure.

The resultant wave field consists of the incident and scattered components (both reflection and transmission).The modeling of damaged cell is similar to that of typical one for modes extraction except that additional interior dofs might be included. The coupling condition is governed by the dynamics equation of coupling structures that can be condensed as

$$\begin{bmatrix} \mathbf{S}_{ll}^{c} & \mathbf{S}_{lr}^{c} \\ \mathbf{S}_{rl}^{c} & \mathbf{S}_{rr}^{c} \end{bmatrix} \begin{Bmatrix} \mathbf{q}_{l}^{c} \\ \mathbf{q}_{r}^{c} \end{Bmatrix} = \begin{Bmatrix} \mathbf{F}_{l}^{c} \\ \mathbf{F}_{r}^{c} \end{Bmatrix}. \tag{8}$$

Considering the couple conditions

$$\mathbf{q}_{l}^{c} = \left[\mathbf{q}^{+}\right]\mathbf{A}^{inc} + \left[\mathbf{q}^{-}\right]\mathbf{A}^{ref}, \quad \mathbf{q}_{r}^{c} = \left[\mathbf{q}^{+}\right]\mathbf{A}^{tra}, \tag{9}$$

and

$$\mathbf{F}_{l}^{c} = \left[\mathbf{F}^{+}\right]\mathbf{A}^{inc} + \left[\mathbf{F}^{-}\right]\mathbf{A}^{ref}, \quad \mathbf{F}_{r}^{c} = \left[\mathbf{F}^{+}\right]\mathbf{A}^{tra}, \tag{10}$$

the governing equations for the scattering problem can be obtained from eq. 7 :

$$\begin{bmatrix} \mathbf{S}_{ll}^{c}\left[\mathbf{q}^{-}\right] - \left[\mathbf{F}^{-}\right] & \mathbf{S}_{lr}^{c}\left[\mathbf{q}^{+}\right] \\ \mathbf{S}_{rl}^{c}\left[\mathbf{q}^{-}\right] & \mathbf{S}_{rr}^{c}\left[\mathbf{q}^{+}\right] + \left[\mathbf{F}^{+}\right] \end{bmatrix} \begin{Bmatrix} \mathbf{A}^{ref} \\ \mathbf{A}^{tra} \end{Bmatrix} = \begin{bmatrix} \left[\mathbf{F}^{+}\right] - \mathbf{S}_{ll}^{c}\left[\mathbf{q}^{+}\right] \\ -\mathbf{S}_{rl}^{c}\left[\mathbf{q}^{+}\right] \end{bmatrix} \left\{\mathbf{A}^{inc}\right\}, \tag{11}$$

Given a single or a set of incident modes as the input in Equation 10, scattered modes (reflection and transmission) acting as the output can be obtained. Numerically, the base number Nr is suggested to be frequency dependent, which can be implemented by a routine to include those slightly evanescent wave modes into the bases.

To numerically describe the wave mode scattering, the reflection and transmission coefficients are defined by the solution of response from Equation 11:

$$\mathbf{R}_i = \frac{\mathbf{A}_i^{ref}}{\mathbf{A}_i^{inc}}, \quad \mathbf{T}_i = \frac{\mathbf{A}_i^{tra}}{\mathbf{A}_i^{inc}} \tag{12}$$

where $i = 1, 2, ..., Nr$. It should be mentioned that the coefficients depend not only on the defects, but also on the normalization method of eigenmodes and the size of intact part of waveguide that included for the reduction of high order near-field modes. The change of the phase of the coefficient with the frequency is partially owing to the size of intact part of waveguide in coupling structure model.

3 NUMERICAL IMPLEMENTATIONS

Guided wave techniques have two main objectives: defect localization and defect sizing. The location of the defect can be easily evaluated from the reflection of a well tuned wave packet. Practically, the time frequency analysis or denoise processing of the obtained testing signal is necessary. The sizing of the defects is much more difficult, because the reflection or transmission signal depends not only the defect size or shape, but also the mode type and frequency, potential mode conversion, and the attenuation due to dissipation, leakage or geometry. However, the wave-defect interaction analysis will help to find out which type of modes are sensitive to a given type of defects. Generally, the numerical wave-defect interaction analysis will provide a reference of the sizing in the practical test, at least to some extent.

3.1 Methodology

To construct the database of reflection coefficients, a numerical finite element model of a pipe-damaged section was created. The defect is a rectangular notch with three-dimensional variables: depth, axial and circumferential extents (figure 3). These parameters can describe most of defects types that can be encountred such as (notchs, corrosion, metal loss ...). The pipe is steel with a density $\rho = 7800kg.m^{-3}$, a Young modulus $E = 2.10^{11}Pa$ and a Poisson‘s ratio $\nu = 0.3$. The outer diameter is $168mm$ and the thickness of the pipe wall is $11mm$. Reflection coefficients calculation was made depending on the frequency in the range $[5 - 15]kHz$. This latter corresponds practically to the signal frequency by wich the pipe under test was excited. The torsion mode was considered in the calculation process. In fact, the inspection system use this mode to generate guided waves for the defect detection.

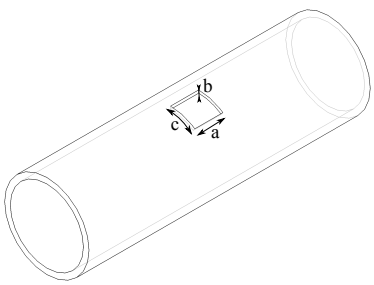

Figure 3: Damaged pipe with defect dimensions.

The waveguide 1 is a pipe section connected to the waveguide 2 wich is a coupling structure with defect and it is in turn connected to waveguide 3 similar to the 1^{st} one (see figure 4). Several iterations conduct us to obtain a database that contain reflection coefficients as a function of four variables : a, b, c and f, respectively, axial, depth, circumferential extents and frequency.

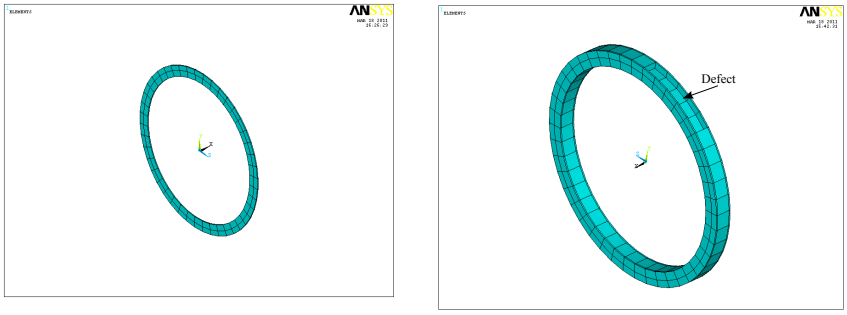

(a) (b)

Figure 4: Finite element models of waveguides : (a) Waveguide 1 and 3, (b) Waveguide 2

3.2 Numerical results and interpretations

Figure 5 shows the reflection coefficients variation with frequency for different defect sizes. These curves prove the dependence of reflection coefficients with the excitation frequency. Generally speaking, these coefficients increase with the frequency. Figure 6 shows the reflection coefficients variation with axial, circumferential and depth defect extents at 10kHz for different sizes. These curves demonstrate the increase of the reflection coefficients with the defect sizes. The database constructed by a large diversity of defect sizes let us to plot the 3-D curves showing the evolution of reflection coefficients with two chosen variables from the defect dimensions (a, b or c) at a given frequency. In figure 7 we can see 3-D graphs of the reflection coefficients variation with defect sizes at $10kHz$. It is clear that the reflection monotonically increases with axial extent at constant depth and vice versa, it also increases with circumferential extent at constant axial extent and vice versa.
Figure 8 shows color maps of the 3-D reflection plot in figure 7. The lines are isolines of constant reflection coefficient as described by the color bar. From these isolines we can observe that the reflection coefficient obtained for example at a certain depth and axial extent is also obtained at smaller depth and larger axial extent.

4 CONCLUSIONS

In this study, the Wave Finite Element Method was used to calculate the reflection coefficients from a rectangular notch, with varying dimensions, located in a pipe excited by torsional mode. The database created will serve for the sizing of defects detected by an experimental inspection system. Results show the increase of the reflection coefficients with the defect sizes and its dependence on the frequency. The reflection coefficients generally have nonlinear relationship with defects size of transverse size except at some frequencies. This means the choice of central frequency is crucial for the accurate estimation of the damage severity.

REFERENCES

[1] A Demma. The reflection of guided waves from notches in pipes: a guide for interpreting corrosion measurements. *NDT & E International*, 37(3):167–180, 2004.

[2] J. Ma, F. Simonetti, and M. J. S. Lowe. Scattering of the fundamental torsional mode by an axisymmetric layer inside a pipe. *The Journal of the Acoustical Society of America*, 120(4):1871–1880, October 2006.

[3] Lon Brillouin. *Wave Propagation in Periodic Structures*. Courier Dover Publications, December 2003.

[4] W. X. Zhong and F. W. Williams. On the direct solution of wave propagation for repetitive structures. *Journal of Sound and Vibration*, 181(3):485–501, March 1995.

[5] M.N. Ichchou, J.-M. Mencik, and W. Zhou. Wave finite elements for low and mid-frequency description of coupled structures with damage. *Computer Methods in Applied Mechanics and Engineering*, 198(15-16):1311–1326, 2009.

[6] W Zhou, M Ichchou, and J Mencik. Analysis of wave propagation in cylindrical pipes with local inhomogeneities. *Journal of Sound and Vibration*, 319(1-2):335–354, 2009.

[7] W.J. Zhou and M.N. Ichchou. Wave propagation in mechanical waveguide with curved members using wave finite element solution. *Computer Methods in Applied Mechanics and Engineering*, 199(33-36):2099–2109, 2010.

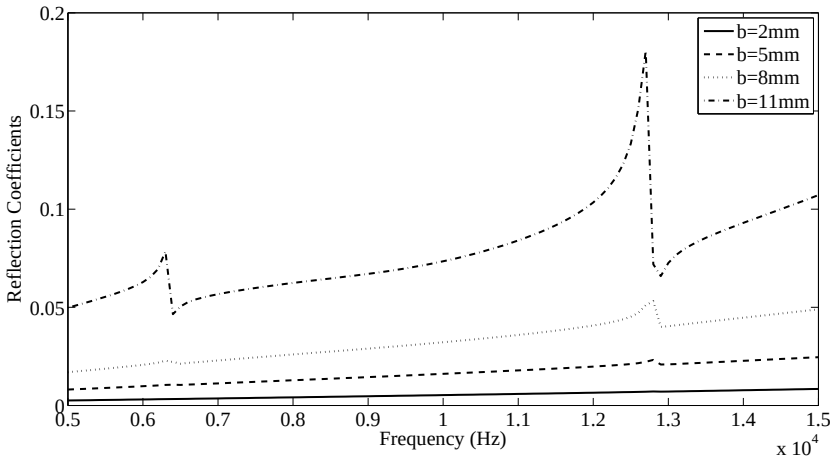

(a)

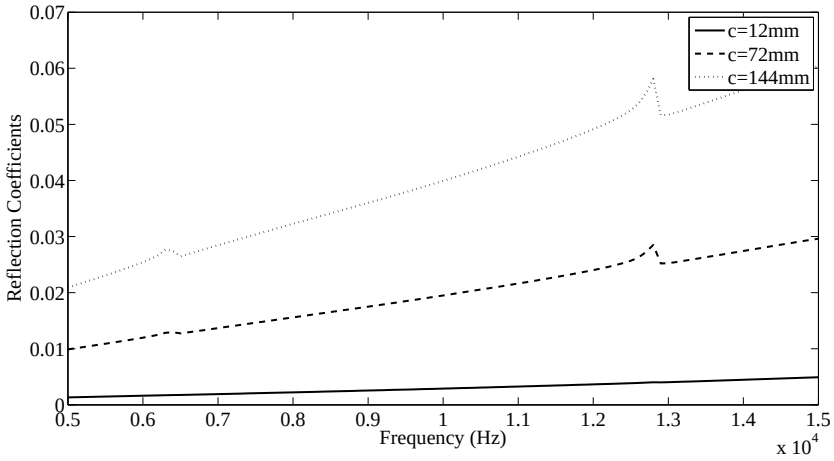

(b)

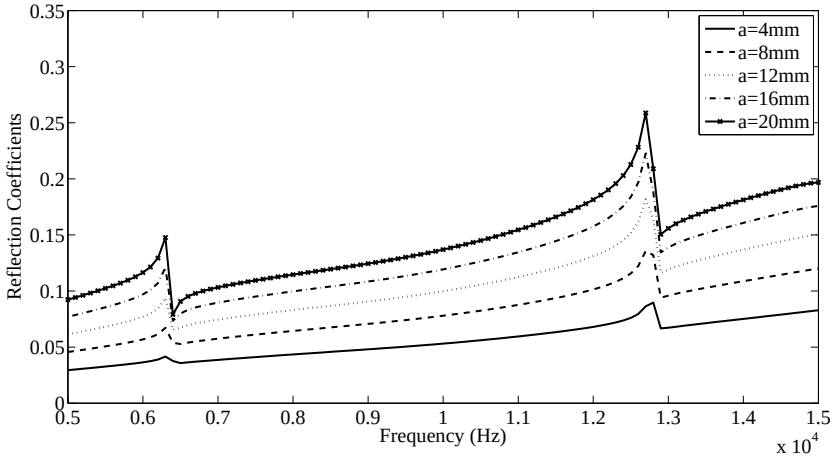

(c)

Figure 5: Reflection coefficients variation with frequency for : (a) different defect depth with $a = 8mm$, $c = 60mm$; (b) different defect circumferential-extents with $a = 8mm$, $b = 5mm$; and (c) different defect axial-extents with $c = 132mm$, $b = 8mm$

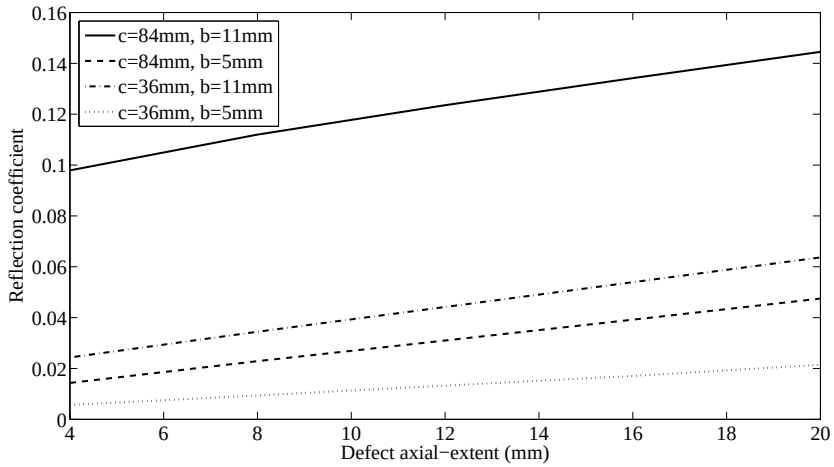

(a)

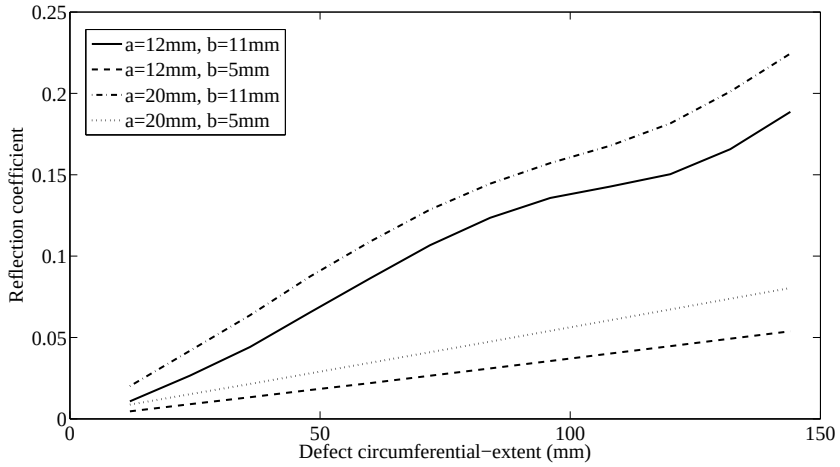

(b)

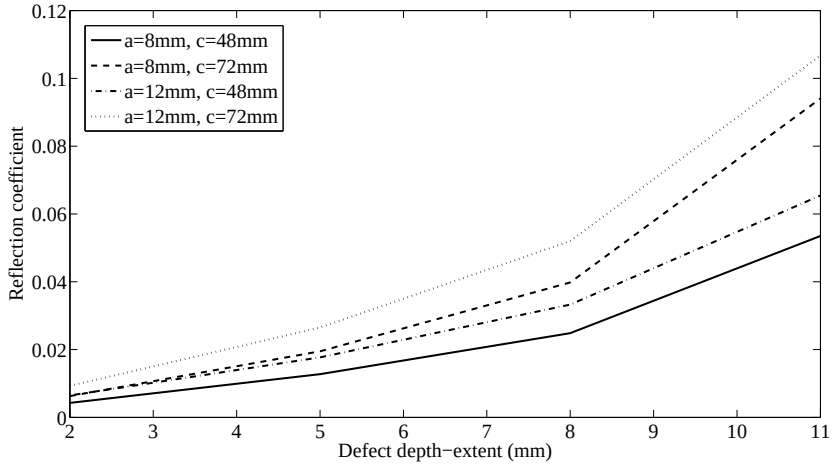

(c)

Figure 6: Reflection coefficients variation with : (a) defect axial-extents for different circumferential and depth sizes; (b) defect circumferential-extents for different axial and depth sizes; and (c) defect depth for different circumferential and axial sizes; at $10kHz$

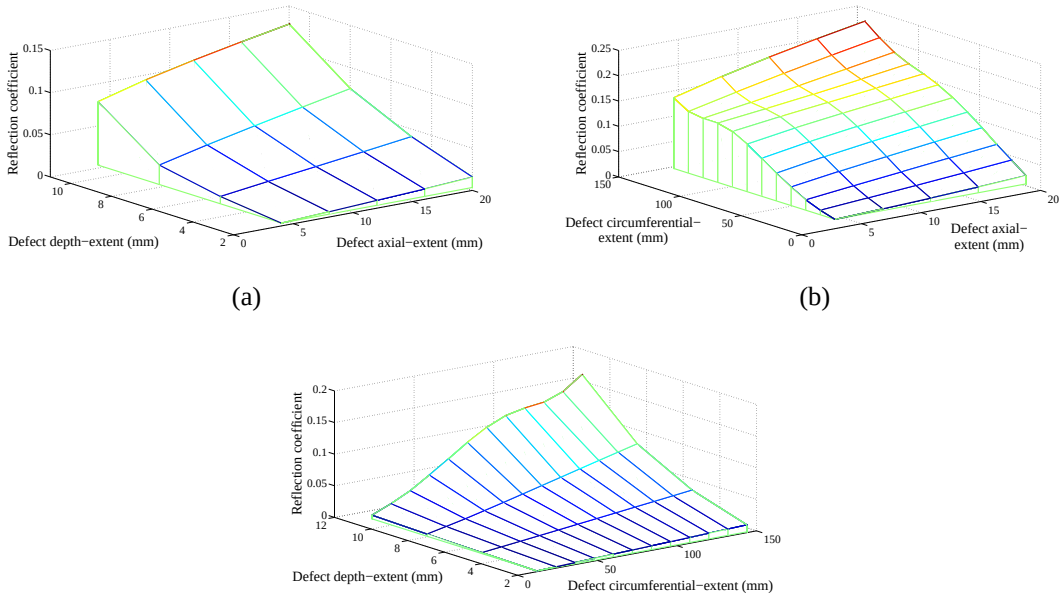

Figure 7: 3D graph of reflection coefficients at $10kHz$ with : (a) varying depth and axial extent $(c = 72mm)$, (b) varying circumferential and axial extents (through thickness defect) and, (c) varying depth and circumferential extent $(a = 8mm)$.

.

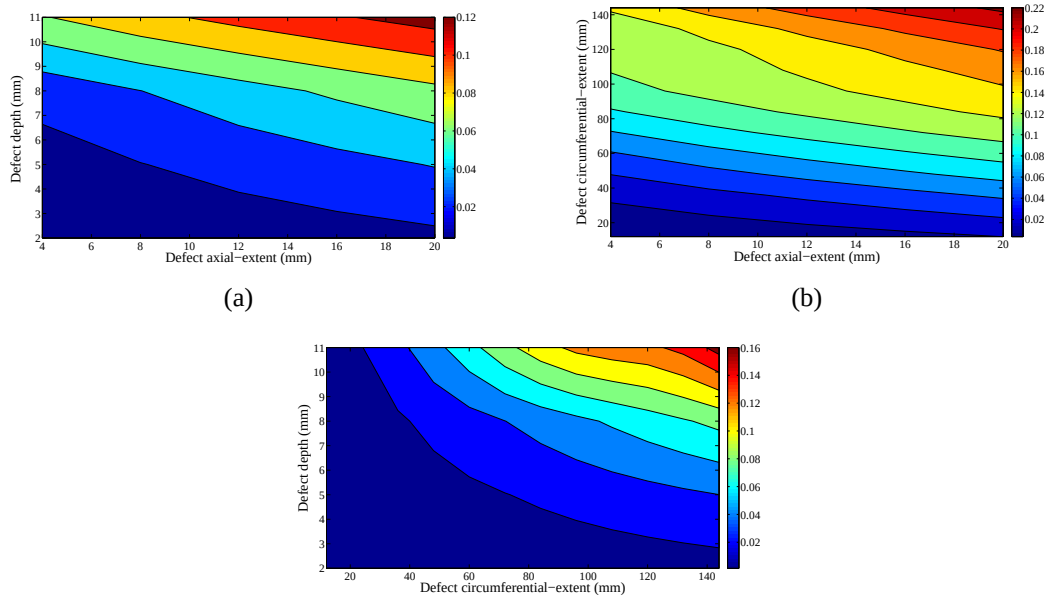

Figure 8: Color map of reflection coefficients at $10kHz$ with : (a) varying depth and axial extent $(c = 72mm)$, (b) varying circumferential and axial extents (through thickness defect) and, (c) varying depth and circumferential extent $(a = 8mm)$.

.